PHYSICAL REVIEW B **73**, 195303 (2006)

Origin of the hole gas at the Si(111):Cl surface: Role of surface electronic structure, impurities, and defects

Torbjörn Blomquist* and George Kirczenow†
Department of Physics, Simon Fraser University, Burnaby, British Columbia V5A 1S6, Canada
(Received 22 December 2005; published 2 May 2006)

A two-dimensional hole gas was found at the Si(111):Cl surface of an *n*-doped silicon substrate in a recent experiment. We investigate this surface theoretically, using a self-consistent Poisson-Schrödinger model, and show that this hole gas is not, contrary to a previously proposed explanation, intrinsic to the ideal Si(111):Cl surface. Our finding is consistent with the *ab initio* electronic band structure. We then examine theoretically a number of defects and impurities that may be expected to be present on this surface and find excess adsorbed chlorine atoms, acting as electronic acceptors, to be the most likely source of the observed hole gas. Further, we present simulations of scanning tunneling microscopy images that show how these excess adsorbed chlorine defects should appear in experiments.

DOI: 10.1103/PhysRevB.73.195303 PACS number(s): 68.43.−h, 73.20.Hb, 68.47.Fg, 87.64.Dz

I. INTRODUCTION

Silicon surfaces have long been studied mainly for their applications in modern microelectronics, but also for use as substrates in various fundamental experiments, most recently in molecular electronics.[1–11]

Chemical modification of semiconductor surfaces is interesting in that it can stabilize a surface and also affect the electronic structure of the surface. The most common surface modification is oxidation; silicon oxide offers a very stable and isolating surface layer. However, this surface is unordered and full of defects when viewed on the nanoscale. Hydrogen termination of silicon surfaces is commonly used in experiments and yields a fairly stable surface that can survive for some time in air and is well ordered. There is no problem of lattice mismatch as with the silicon–silicon oxide interface. Another possible way to terminate a silicon surface is with chlorine. The chlorine terminates the dangling bonds of the "clean" silicon surface in the same way as hydrogen, but due to the much higher electronegativity, i.e., the higher electron-attracting ability,[12] of chlorine, one might expect effects on the electronic surface structure, such as band bending.[13] Indeed, a recent experimental paper on chlorine-terminated silicon (111) surfaces reported the formation of a hole gas at the surface of an *n*-doped silicon substrate and attributed this effect to strong band bending near the Si surface.[14] In this paper, we examine the Si(111):Cl surface theoretically and find that the formation of the surface hole gas cannot be, contrary to the explanation proposed in Ref. 14, due to band bending induced by the high electronegativity of the terminating chlorine. We suggest instead that defects in the form of excess Cl atoms adsorbed on the surface are the most likely source of the hole gas.

In this paper we first introduce and explain a self-consistent Poisson-Schrödinger model that we have developed. We then discuss the ideal Si(111):Cl surface and show that no hole gas can form intrinsically at this surface; this conclusion is based on calculations using our model and also on the results of previous theoretical *ab initio* calculations for this surface as well as previous experimental studies. Having established the fact that the observed hole gas is extrinsic, we move on to examine different defects and impurities at this surface and we find one likely candidate for a shallow acceptor that can create a two-dimensional hole gas at the Si(111):Cl surface, namely, excess Cl atoms that have been ionically adsorbed on the surface. We present a detailed study of the energy levels and wave functions of this acceptor, using our Poisson-Schrödinger model. The stability of this defect is discussed and especially how it is affected by doping of the crystal. We also perform simulations of scanning tunneling microscopy images to investigate how these excess Cl atoms can be observed in experiment.

II. MODEL

We employ a self-consistent Poisson-Schrödinger model for the calculations of the electronic structure. We have used this model in previous studies of charge transfer involving dopants in Si nanoparticles and dangling bonds at Si surfaces,[15–17] but in the present work we have extended it to include more atomic species by use of extended Hückel[18] parameters that have been tailored to yield an accurate description of the silicon-chlorine system. The current model allows for calculations on large systems, containing more than 1000 atoms, while including important electron-electron interactions, making it possible to study single impurities in large clusters.[62] It also reproduces the band structure and band gap of silicon with high precision; few other models allow for high-precision band structure—density functional theory for example produces a band gap for silicon that is a factor 2 too small.[19] The present model has been specifically tailored for examining silicon structures with impurities and surface modifications. See our previous publications, Refs. 15–17, for how it has been validated by comparisons to *ab initio* calculations and experiments. The model is validated further in this paper specifically for Cl-terminated surfaces by comparison with previous *ab initio* calculations. Briefly, the self-consistent model works as follows. The wave functions of all valence electrons are calculated in a tight-binding model. The electrostatic potential and on-site electron repul-

 ©2006 The American Physical Society

sion using experimental valence orbital ionization energies[20] (VOIEs) is then calculated and used in the next iteration to adjust on-site potentials.

The on-site potentials are based on VOIEs.[20] The on-site potential of an orbital of type $l \in \{s,p,d\}$ on site i is given as

$$H_{il} = A_l p_{il} + B_l + C_l q_i - eV_i, \tag{1}$$

where A_l, B_l, and C_l are fitting parameters found in Ref. 20. The population of the orbital is $0 \leqslant p_{il} \leqslant 2$, q_i is the total charge on the atom, e is the elementary charge, and V_i is the electric potential at the site. This functional form for the on-site potentials is used for all atomic species except hydrogen, which uses an s basis with the on-site potential

$$H_i = 0.121 q_i^3 - 13.97 q_i^2 - 26.93 q_i - 13.6 - eV_i, \tag{2}$$

expressed in eV and based on the valence orbital ionization energy for the charge dependence.[20]

We use extended Hückel for overlap integrals and hopping, between all elements except for Si-Si, Si-P, and Si-Al, for which we have a special model that is optimized to reproduce the band structure of silicon with precision.[15–17] The extended Hückel hopping energies are calculated as

$$H_{ij} = k' S_{ij} \frac{H_{ii} + H_{jj}}{2}, \tag{3}$$

$$k' = k + \Delta^2 + \Delta^4(1-k), \tag{4}$$

$$\Delta = \frac{H_{ii} - H_{jj}}{H_{ii} + H_{jj}}, \tag{5}$$

where k is a fitting constant,[21] often chosen to be 1.75.[18]

The overlap integrals S_{ij} of the Slater orbitals are calculated using the standard Hückel parameters. The angular dependence is the standard Slater-Koster form[22] and the radial dependence is calculated using an algorithm by Guseinov.[23] The overlaps of orbitals centered on atoms more than 12.5 a.u. apart are eliminated by the use of a cutoff function, see Refs. 17 and 24

In order to reproduce, with precision, the band structure of silicon, we use an s, p, and d basis and special hopping and overlap parameters for silicon, originally developed by Bernstein *et al.*,[24] but adapted for use with a Poisson-Schrödinger model.[17] In order to align the orbitals with the standard Hückel parameters, we have shifted the energy levels of this tight-binding model by

$$H'_{ij} = H_{ij}\left(-e\frac{V_i + V_j}{2} - 1.04 \text{ Ry}\right) S_{ij}, \tag{6}$$

where S_{ij} is the overlap matrix element, and V_i is the electrostatic potential at the atom that orbital i is centered on. Since aluminum and phosphorus are isoelectronic, we use the same hopping and overlap parameters as for silicon when Al and P are substitutional impurities in Si. The on-site energies, however, are based on VOIE data, together with a fit for the B_l parameters (see Ref. 17 for details). The overlap matrix elements between Si orbitals can be found in Ref. 24.

To obtain the wave functions and corresponding eigenenergies, we solve the Schrödinger equation

$$H\psi = ES\psi. \tag{7}$$

To complete the Poisson-Schrödinger model, we self-consistently solve the tight-binding model and the electrostatic potential, by populating all the states below the Fermi level with electrons. For nonzero temperature, a Fermi-Dirac distribution may be used. The details of how the electrostatic potential is calculated can be found in Appendix A of Ref. 17. In short, the electrostatic potential at an atomic site is the sum of the Coulomb potentials from all other sites. The charge on each site is calculated using Mulliken population analysis.[20] Our model is similar to the one used by Lannoo *et al.*[25]

III. THE Si(111):Cl SURFACE

The chlorine-terminated silicon surface has been studied for quite some time, both experimentally and theoretically.[26–51] Early work was centered on deciding the binding sites for the chlorine.[26–37] Two possibilities were considered, covalent binding to the top silicon atoms and ionic binding with the chlorine in a threefold site. Comparison between photoemission spectra and theoretical calculations of the electronic structure indicated the covalent position.[26–34] This was later confirmed by scanning tunneling microscopy studies.[38] These experiments and *ab initio* calculations give a detailed picture of the electronic structure of the Si(111):Cl surface; they are also in good agreement with each other. The addition of chlorine to the surface creates bands that can be attributed to the chlorine σ and π orbitals.[27–30] There is also a band that stems from the Si-Si bonds between the two top Si layers; these states have been modified by the presence of the chlorine.[28–30] All of these surface bands are, however, below the valence band edge and the chlorine adds exactly the right number of electrons to fill these states.[27–31] Consequently, the valence band is completely filled while the conductance band is empty and the band gap is unchanged from the bulk value. This is an electronically inert surface and no electron or hole gas can form intrinsically at this surface.

We have performed calculations on infinite slabs containing 80 atomic layers of silicon, with Si(111) surfaces terminated with hydrogen or chlorine. Our calculations agree with earlier *ab initio* calculations,[29–31] but we examine here in more detail the potential profile and the effects of any band bending at the Si(111):Cl surface. We then consider a variety of possible surface defects as the potential source of the hole gas that has been observed experimentally.

Figure 1 shows the Mulliken charge and the electric potential at the different atomic sites, as function of the sites' z coordinates, in two Si slabs containing 80 Si layers and terminated by either chlorine or hydrogen. Electronegativity is a measure of an atom species' ability to attract (negative) electric charge. The electronegativities of Si, H, and Cl are 1.8, 2.1, and 3.0, respectively.[52] The Si-Cl bond is therefore much more polarized than the Si-H bond with the Si atom being positively charged in both cases (see Fig. 1). The Si-H or Si-Cl bonds create an electric dipole layer at the surface, which shifts the electric potential inside the Si slab with respect to the vacuum level. The charge on other sites than

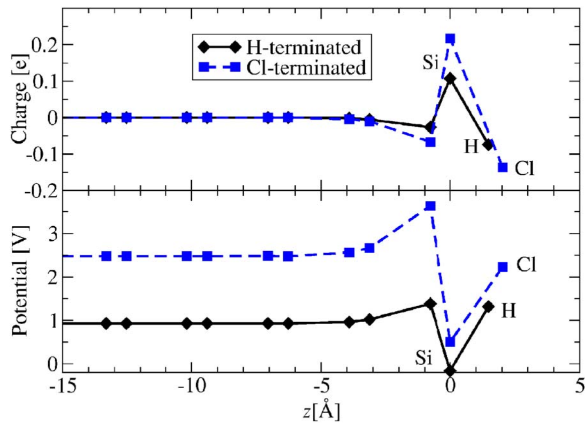

FIG. 1. (Color online) Upper panel: The Mulliken charge on the different atomic sites, as function of the sites' z coordinates, in two Si slabs containing 80 Si atom layers (only ten shown) and terminated by Cl [(blue) dashed curve] or H [(black) solid curve]. All sites are Si sites unless otherwise marked. Lower panel: The electric potential on the same atomic sites. The electric potential inside the Cl-terminated slab is ≈ 1.55 V higher than in the H-terminated slab, due to the larger polarization of the Si-Cl bond.

the surface Si layer and the terminating Cl sites is small and we can see that the electrostatic potential is nearly constant from the third Si layer on into the slab. The term "band bending" can be somewhat misleading in this case, because the potential shift from the vacuum level happens on a length scale that is much smaller than the length scale of effective mass theory from which the band bending concept originates.[13] The electrostatic potential is constant on a length scale relevant to effective mass theory but with a constant shift from the vacuum level; we will therefore refer to this as band shift. We note that the bands are shifted to lower energy (higher electrical potential) and if it would be possible for charge to move from another part of the semiconductor, perhaps a surface with different termination, we would expect an accumulation of electrons near this surface, not holes.

Figure 2 shows the on-site Mulliken probabilities of the valence band top wave function in Si slabs terminated with H or Cl. In both cases we see sinusoidal wave functions typical of flat potentials; a small influence of the termination can be seen at the boundaries of the wave function.

We find the valence band edge in the Cl-terminated slab to be 1.55 eV lower than in the H-terminated slab, in good agreement with the potential seen in Fig. 1 and also the difference in work function measured by Lopinski *et al.*,[14] i.e., 1.2–1.5 eV.

The valence band edge is clearly a bulk state; we find all surface states related to the Cl termination to be below the valence band edge. With both H and Cl termination, all calculations yield the full silicon bulk band gap with any surface bands either above the conduction band edge or below the valence band edge, in agreement with previous *ab initio* calculations.[27,30] We find the band gap widening due to the finite size of the 80 Si layer slab to be less than 10 meV. It is very clear from our calculations and the above-mentioned earlier theoretical *ab initio* and experimental results that the observed hole gas cannot be intrinsic to the ideal Si(111):Cl surface.

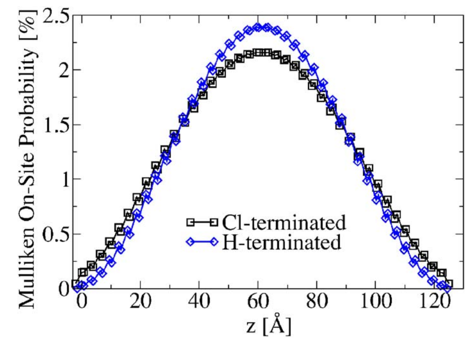

FIG. 2. (Color online) On-site Mulliken (Ref. 20) probability distributions of the wave functions of eigenstates at the top of the valence band vs site z coordinate in Cl-terminated [(black) squares] and H-terminated [(blue) diamonds] Si slabs containing 80 Si layers. Both curves are as expected for sinusoidal wave functions associated with flat potentials, but the Cl-terminated slab displays noticeable deviations from this behavior very near to the boundaries.

To conclude, we find, consistent with previous theoretical work, that the Cl termination does not create any surface states in the band gap and leaves the Si bands flat, although shifted with respect to the vacuum level. No electron or hole gas can therefore form intrinsically at a Cl-terminated surface. The low density of the hole gas, one hole per 1280 Cl atoms, observed by Lopinski *et al.*,[14] further supports that it is of extrinsic nature. The difference in work function between H- and Cl-terminated surfaces measured by Lopinski *et al.* is due to the different polarizations of the Si-H and Si-Cl bonds.

IV. POSSIBLE IMPURITIES AND DEFECTS

With the conclusion that the hole gas observed by Lopinski *et al.* is not intrinsic to an ideal Si(111):Cl surface, we carried out a series of calculations directed at identifying possible impurities or defects that may create a hole gas. The defects and impurities that we studied were investigated by calculations on silicon crystallites, shaped as half spheres with a Si(111):Cl surface and a H-terminated back surface.

Before we start analyzing the different impurities and defects, we need to consider how localized impurity levels are affected by the finite size of the crystallites investigated here, in order to be able to draw conclusions about the properties of the corresponding levels associated with macroscopic surfaces. We consider the bound state wave function related to a defect or impurity with an eigenenergy in the band gap of the semiconductor, but close to a band edge. This wave function is a linear combination of the relevant bulk band edge wave functions. In a finite crystallite, the impurity wave function is confined and this causes the energy level of the impurity state to move further into the band gap (the band gap is also widened by the finite size).[17] Consequently, if we find a defect or impurity state near a band edge in a small crystallite, we will find it even closer to this band edge in a macroscopic sample. Generally, the energy of an impurity state in the band gap can be fitted to a function

$$E = E_0 + Ar^{-2}, \quad (8)$$

where E is the energy of the state relative to the relevant band edge, r is the radius of the crystallite, and E_0 and A are fitting parameters.[17] This allows us to estimate the energy level of a defect or impurity in a macroscopic sample by performing calculations on crystallites of different sizes and then extrapolating to infinite size. The r^{-2} power law can most easily be understood in the effective mass approximation; consider a particle in a box.

We have also previously analyzed the wave function within the silicon of a defect (a dangling bond) on a H-terminated silicon surface in the effective mass approximation and found this approximation to work well beyond a distance of 7 Å from the defect site.[16]

A. Dangling bond defect

In the present Si(111):Cl system, a dangling bond is formed at the surface when a terminating Cl atom is missing. Such a nonterminated site is also referred to as a radical surface site. Radicals have unpaired electrons and are known from chemistry to be extremely reactive. The dangling bond can, however, be stabilized if an extra electron can be supplied, e.g., from the bulk of the silicon. We find, however, that the radical surface site on Cl-terminated silicon has similar electronic properties and essentially the same energy levels as on H-terminated silicon, which we have investigated earlier.[16] The dangling bond forms a level inside the band gap, but it is a deep acceptor, near the center of the band gap. Valence band electrons cannot to a significant degree be thermally excited into this state and it can therefore not be creating the observed hole gas. For details, we refer to Ref. 16, since the present results are very similar to those for the Si(111):H surface studied there.[63]

B. Cl in bridging position

Chlorine is known from studies of the Si(100) surface to be able to break up Si-Si bonds and enter into a bridging position between Si atoms.[51] Figure 3 shows a Cl atom in such a bridging position on the Si(111):Cl surface. We have obtained the geometry by a semiempirical calculation on the crystallite shown in Fig. 3.[53] Employing our Poisson-Schrödinger model for this geometry, we find that the bridging Cl atom creates a donor state 183 meV below the conduction band, in a small 119-Si-atom crystallite with a 2.7 eV band gap (see Fig. 3). As explained at the start of Sec. IV, we can expect this donor state to be quite shallow for a large silicon substrate.

C. Interstitially absorbed Cl

Substitutional chlorine is known to be a donor, but interstitial chlorine (see Fig. 4) is an acceptor.[54] An acceptor level of 270 meV has been measured,[55] but it may be modified if the interstitial position is near the surface. Chlorine in bulk positions would not create a two-dimensional hole gas at the surface and also the mobility of Cl in silicon is very low due to the size of Cl atoms. However, chlorine is known to etch

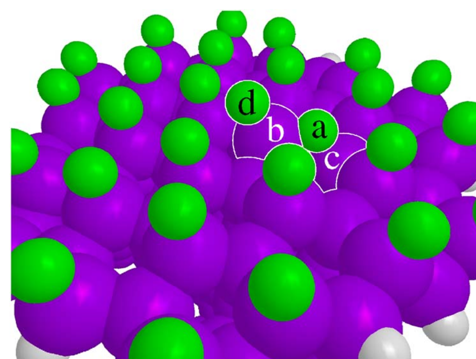

FIG. 3. (Color online) A silicon crystallite with a Si(111):Cl surface. The Cl atom (green) marked a is in a bridging position between Si atoms marked b and c. The presence of the bridging Cl atom displaces the Si atom (purple) marked b and the Cl atom marked d while the displacement of other atoms is quite small. A chlorine defect of this kind is a shallow donor.

Si(111) surfaces.[14,50] This happens in two steps. First a chlorine atom is absorbed into the void below a silicon atom in the top layer of the surface (this is an endothermic reaction, but the uv light used by Lopinski *et al.*[14] is sufficiently energetic); this reduces the binding energy of the silicon atom which can then more easily be removed.[50] If the reaction terminates after the first step, we are left with a subsurface interstitial Cl atom.

We used our Poisson-Schrödinger model to calculate the energy of the acceptor state of interstitial chlorine at the center of seven H-terminated spherical silicon crystallites, ranging from $Si_{124}H_{72}Cl$ to $Si_{476}H_{172}Cl$. Extrapolation of the acceptor energy to infinite crystal size, using Eq. (8), yields a value of $E=235$ meV, in good agreement with the experimental value (270 meV). We repeated this procedure with crystallites formed as half spheres with a Si(111):Cl surface, a H-terminated back surface, and a subsurface interstitial Cl impurity at the center of the Cl surface. The 18 crystallites used ranged from $Si_{40}H_{30}Cl_{11}$ to $Si_{534}H_{183}Cl_{74}$ and yielded an extrapolated value of the acceptor state of $E=565$ meV. Although the electric potential at this position is more positive than at an interstitial bulk position, the acceptor level is very

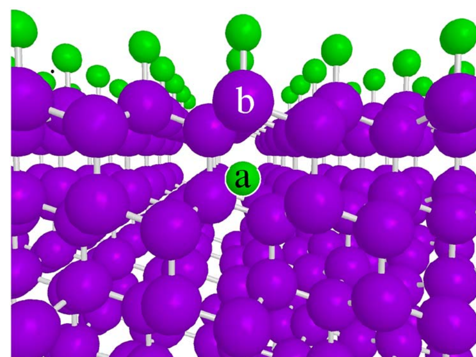

FIG. 4. (Color online) Cutout of Si crystal with Si(111):Cl surface, showing the position of the interstitial Cl atom. The interstitial Cl atom (green) is marked by a and is in a position straight below the Si atom (purple) marked b, at the center of a void in the lattice.

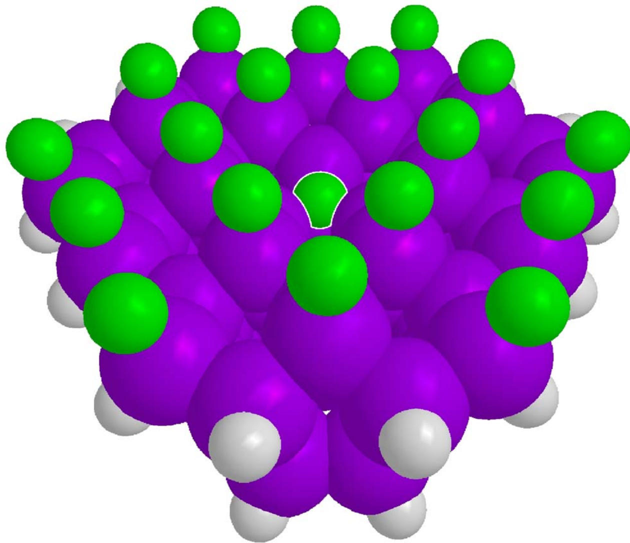

FIG. 5. (Color online) Model for Si(111):Cl surface with a minimal etch pit. A Cl atom (green) is seen at the center of the etch pit on the top Si(111) surface terminated with Cl atoms (green). The back surface of the crystallite is terminated with hydrogen (white). (Silicon atoms are purple.)

deep and this acceptor, like the dangling bond, cannot be thermally excited to a significant degree.

D. Minimal etch pit with one Cl atom

As mentioned above, chlorine can etch silicon,[14,50] and when one top-layer Si atom is removed from the surface, a minimal etch pit is formed. The chlorine atom that assists the etching is left at the center of the etch pit (see Fig. 5).[50] We used our model to calculate the electronic character of this surface defect and found it to be a double donor. We observe a 3.2 eV band gap and we find the donor level for the first electron to be 87 meV from the conduction band edge, in a small $Si_{79}H_{49}Cl_{20}$ crystallite geometry optimized by a semiempirical method[53] (see Fig. 5). As with the Cl in the bridging position, following the explanation at the start of Sec. IV, we can expect this defect to be a shallow donor for a large silicon substrate. Donating the first electron requires very little energy but to donate the second electron much more energy is required.

E. Minimal etch pit with two Cl atoms

In a minimal etch pit, the absent Si atom leaves three dangling bonds on three atoms in the second atom layer. It is possible for two Cl atoms to sit in the minimal etch pit. One creates a bridging bond between two of the unterminated Si atoms while the other Cl atom terminates the third dangling bond (see Fig. 6). The bridging Cl atom creates a single shallow donor state just like the bridging Cl atom earlier in the paper. The $Si_{79}H_{49}Cl_{21}$ crystallite used to model this etch pit has a band gap of 3.0 eV and a single donor state 114 meV below the conduction band. We can, therefore, following the examples of the Cl in bridging position and the etch pit with one Cl atom, expect this defect to be a very shallow donor for a large silicon substrate.

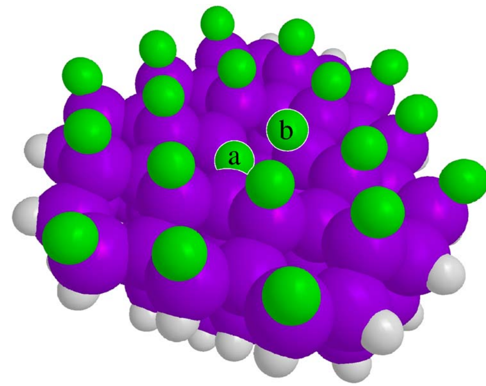

FIG. 6. (Color online) Model for Si(111):Cl surface with a minimal etch pit. Two Cl atoms (green) are seen in the etch pit on the top Si(111) surface terminated with Cl atoms (green). The Cl atom marked *a* is in a bridging position, while the Cl atom marked *b* terminates the third dangling bond of the etch pit. The back surface of the crystallite is terminated with hydrogen (white). (Silicon atoms are purple.)

F. Surface-adsorbed excess Cl

Chlorine has a very high electronegativity and can take an electron from the substrate and form an ionic bond. This allows for a small amount of excess chlorine to bind to the surface at threefold sites. We found, however, for small crystallites, *n*-doping the crystallite to be necessary for such bonding to be energetically stable; otherwise, the excess Cl atom will cause a rearrangement of the surface which results in a Cl atom occupying a bridging position (see Sec. IV B and Fig. 3). However, these small crystallites have a much larger band gap than bulk silicon due to confinement effects and we know from our previous work that it is mainly the valence band edge that moves down in small crystallites while the conduction band edge remains the same as in bulk.[15,17] It may therefore be possible, and we will show below that it is, for larger crystallites with smaller band gaps to bind an excess chlorine atom without *n* doping. We performed geometry optimization on a $Si_{118}PH_{63}Cl_{28}$ crystallite to obtain the geometry of the adsorption site for excess chlorine[53] (see Fig. 7 and Table I); the substitutional phosphorus impurity is situated near the bottom of the crystallite and is not visible in the figure. We also modeled larger crystallites based on the geometry optimization of this small crystallite, taking into account the placement of the 15 neighbor and next-neighbor Si atoms to the impurity as well as the six Cl atoms bound to these Si atoms.

We investigated 20 crystallites ranging in size from $Si_{43}H_{28}Cl_{12}$ to $Si_{763}H_{222}Cl_{90}$. The band gap and the energies of three highest occupied states are shown in Fig. 8. These states are found in all of the crystallites: one impurity state localized to the Cl impurity, one twofold-degenerate delocalized bulk state, and a nondegenerate delocalized bulk state. In Fig. 8, we have used the twofold delocalized bulk state as reference energy (black solid line). Notice that the localized

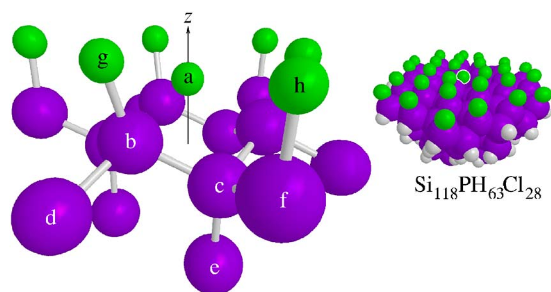

FIG. 7. (Color online) Geometry of the Cl-atom adsorption site. The left panel shows the atoms near the adsorption site whose positions have been altered by the presence of the excess Cl atom, marked a. The positions of these atoms are shown in Table I. The right panel shows the $Si_{118}PH_{63}Cl_{28}$ crystallite used for the geometry optimization.

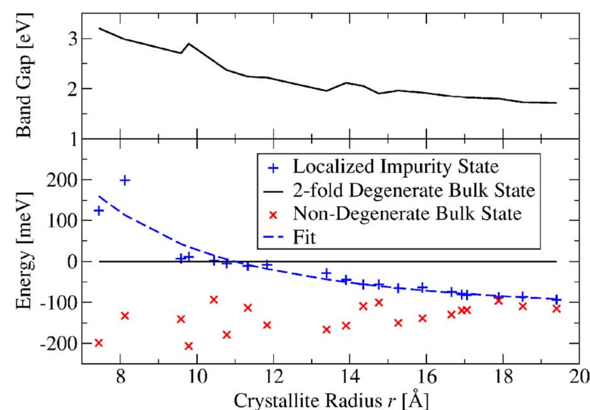

FIG. 8. (Color online) Upper panel: The band gap of different half-sphere-shaped Si crystallites with an excess Cl atom adsorbed on the center of their Si(111):Cl surface, as function of the crystallite radii. Lower panel: The energies of the three highest occupied states, the localized impurity state, shown as (blue) plus signs, and the nondegenerate delocalized bulk state, shown as (red) crosses, relative to the energy of the highest occupied (twofold-degenerate) delocalized bulk state, shown as (black) solid line (by definition zero energy). The states were identified by visual inspection of the wave functions. The function $E=Ar^{-2}+E_0$ has been fitted to the localized impurity state, (blue) dashed curve.

impurity state has a higher energy than the bulk states for small crystallites but the level moves below the twofold-degenerate bulk state for sufficiently large crystallites. At zero temperature and for small crystallites, the localized impurity state has a single occupation. But it will have double occupation for larger crystallites, when the localized impurity state is below the bulk state. The twofold-degenerate bulk state is fully occupied (four electrons) in the small crystallites but one electron is moved to the localized impurity state in the large crystallites.

In the small crystallite ($Si_{118}PH_{63}Cl_{28}$) used for geometry optimization of the impurity site, we had to resort to n doping to obtain stable adsorption of the Cl atom to the threefold site. The n doping assures that the localized impurity state is fully occupied, creating an ionic bond that is energetically stable against a transition of the Cl atom to the bridging position mentioned above. However, for larger crystallites, we can see that doping is not required to ensure that the localized impurity state is fully occupied and we conclude that the Cl atom will be stably adsorbed on the threefold site without doping. Unfortunately, due to practical computational limitations, we cannot perform geometry optimizations on such large systems.

TABLE I. The relaxed geometry of the excess-Cl-atom adsorption site. The geometry is shown in Fig. 7. Numbers within parentheses are the positions of the lattice in the absence of the excess Cl atom. Positions are given in cylindrical coordinates; the z axis is defined in Fig. 7. The adsorption site has a triangular geometry and the ϕ coordinates of the atoms are left unchanged.

Label	Species	ρ (Å)	z (Å)
a	Cl	0.0	1.38
b	Si	2.18 (2.22)	0.18 (0.0)
c	Si	2.23 (2.22)	−0.73 (−0.78)
d	Si	4.38 (4.43)	−0.82 (−0.78)
e	Si	2.21 (2.22)	−3.08 (−3.13)
f	Si	4.41 (4.43)	0.12 (0.0)
g	Cl	2.92 (2.22)	2.14 (2.03)
h	Cl	4.46 (4.43)	2.14 (2.03)

We have fitted the energy for the localized impurity level in the different crystallites to Eq. (8) [see (blue) dashed line in Fig. 8]; the parameters are $A=16\,342.9$ meV Å^2 and $E_0=-135.3$ meV. This allows us to estimate, by extrapolation, that the localized impurity state will reside 135 meV below the highest occupied level in macroscopic silicon substrates.

The energy levels and wave functions evolve quite smoothly from crystallite to crystallite when we increase the size, at least for crystallites with more than 100 Si atoms. It is this that allows us to perform extrapolations such as the one above. It follows that for a macroscopic substrate, we will have a hole in the valence band that is bound to the impurity as the impurity is negatively charged, i.e., the bound acceptor state. The state that will evolve into the acceptor state (for large crystallites, $r>12$ Å) is the partly occupied delocalized state; it simply remains the highest (half) occupied state. The size of the acceptor state for macroscopic substrates is larger than the crystallites examined here (we compute the Bohr radius below); it thus appears completely delocalized in these crystallites. Although the next delocalized state [(red) crosses in Fig. 8] does not evolve smoothly enough with size in these small crystallites to allow fitting to a function, we see a tendency toward smoother behavior and smaller (negative) energies. We can set an upper limit for the energy difference between this state and the partly localized state (that will evolve into the bound hole state) of 100 meV by looking at the largest clusters. This is a higher energy level than we find for the localized state [(blue) crosses and (blue) dashed curve in Fig. 8]. We can therefore draw the conclusion that the second occupied delocalized state [(red) crosses] will evolve into the highest fully occupied and delocalized level in a macroscopic substrate, i.e., the valence band top. The localized impurity state will be below the valence band edge. The upper limit of 100 meV for the energy

difference between the partly occupied state and the fully occupied delocalized state is thus an upper limit for the binding energy of the acceptor state in a macroscopic substrate.

We can also estimate the acceptor state energy for a macroscopic crystal surface within the effective mass theory. We have a negative charge on the surface, which will be dielectrically shielded with an effective relative permittivity of $\epsilon_r = (11.8+1)/2$.[56] The wave function has to go to zero on the surface of the substrate and thus the ground state wave function inside the substrate is that of a hydrogenic p state. The nodal plane of the hydrogenic p state wave function is at the surface and the hydrogenic p state wave function is only valid inside the substrate; the wave function is zero outside. The energy of this hydrogen-atom-like state is[57]

$$E = -\frac{me^4}{8\epsilon_r^2\epsilon_0^2 h^2 n^2} = -45 \text{ meV}, \tag{9}$$

where $m=0.54m_e$ is the mass of the heavy hole[58] and we are restricted to $n=2$ since we have a p state. The corresponding Bohr radius is $r=\epsilon_r\epsilon_0 h^2 n^2/\pi m e^2 = 25$ Å, which is somewhat larger than the crystallites investigated here. Since the effective mass theory does not include central cell corrections the 45 meV binding energy that it yields can be regarded as a lower bound for that of the shallow surface acceptor state, although since the state involved is a p state with a node in the central cell, large central cell corrections are not expected.

V. SCANNING TUNNELING MICROSCOPY SIMULATION

We have performed simulation of scanning tunneling microscopy (STM) images of the Si(111):Cl surface with an excess adsorbed Cl atom. We used a $Si_{664}H_{189}Cl_{75}$ crystallite to model the surface. The tunneling current is calculated in a way very similar to that of Tersoff and Hamann,[59] but we use a different expression, adapted from Landauer-Bütticker formalism, to take into account the populations of states in the substrate and tip.[60] The transmission is calculated using the Fermi golden rule. The current is, in adoption from Tersoff and Hamann,[59] by first-order perturbation

$$I = \frac{2e}{h}\sum_{\alpha\beta}[f(E_\alpha - \mu) - f(E_\beta + eV - \mu)]|M_{\alpha\beta}|^2\delta(E_\alpha - E_\beta), \tag{10}$$

where α and β enumerate the eigenstates in the substrate and the tip, respectively, E_α is the energy of state α, V is the tip bias, $M_{\alpha\beta}$ is the matrix element between states α and β, μ is the Fermi energy in the substrate, and $f(E)$ is the Fermi-Dirac function. The wave functions in the substrate are expanded as

$$|\alpha\rangle = \sum_i A_{\alpha i}|i\rangle, \tag{11}$$

where i enumerates all the atomic orbitals $|i\rangle$ on all atoms in the substrate.

We model the tip using only one atom and we therefore have to make some assumptions about the wave functions at the tip. We assume that the tip is metallic, with a continuum of energies for the eigenstates. Further, we need to make some assumptions about the character of these wave functions on the tip atom, i.e., what the wave functions are on the tip atom; we make the simplest possible assumption, that for each eigenenergy of the substrate there exist n eigenfunctions in the tip, each with a pure atomic orbital character (s, p, or d) on the tip atom, i.e., all terms but one vanish in an expansion of the wave function at the tip in atomic orbitals,

$$\sum_{j'} |j'\rangle\langle j'|\beta\rangle = c_\beta|j\rangle. \tag{12}$$

Here j denotes the atomic orbitals on the tip atom and c_β is a constant. Note here that although we use a nonorthogonal basis, the atomic orbitals on one site are orthogonal to each other and our tip has only one site; thus, all $|\beta\rangle$ are orthogonal. We reenumerate the states $|\beta\rangle$ as $|E,j\rangle$ according to energy and atomic orbital character on the tip atom and take into account the surface density of states $\rho(E)$ of the tip material, and we let n be the number of atomic orbitals on the tip atom,

$$\langle j'|\beta\rangle = \langle j'|E,j\rangle = \delta_{j'j}\sqrt{\frac{\rho(E)}{n}}, \tag{13}$$

which trivially satisfies Eq. (12). The index β in Eq. (10) is then substituted by energy E and index j. The matrix element in Eq. (10) is calculated as

$$M_{\alpha E j} = \langle\alpha|H|E,j\rangle. \tag{14}$$

In calculating the hopping elements between the tip atom and the substrate, we assume that the energies of the tip atomic orbitals remain at their standard extended Hückel values. Equation (10) can then be written as

$$I = \frac{2e}{h}\sum_{\alpha j}[f(E_\alpha - \mu) - f(E_\alpha + eV - \mu)]\frac{\rho(E_\alpha)}{n}\left|\sum_i A_{\alpha i}H_{ij}\right|^2. \tag{15}$$

We model our tip by a tungsten atom with a basis of nine atomic orbitals (s, p, and d). The surface density of states is approximated by the Fermi energy value for the W(100) surface, $\rho(E)=0.75$ at.$^{-1}$ eV^{-1}.[61]

In the simulation, we set a bias V and adjust the height z of the tip atom above the substrate so that a chosen current I is achieved. We then make a plot of z as function of the surface coordinates, to simulate the constant current mode of STM imaging.

Figure 9 shows simulated STM images of the Si(111):Cl surface with an excess adsorbed chlorine atom; see also Fig. 10 for an illustration of the actual positions of the atoms on the surface. The excess chlorine atom is not directly visible in the STM simulations but some effects of its presence are. The Fermi level is very close to the valence band edge, as the excess chlorine atom creates a shallow acceptor state. In the experiment by Lopinski *et al.*,[14] the substrate was n type, putting the Fermi level near the conduction band edge in the bulk, but the existence of a two-dimensional hole gas at the surface shows that the Fermi level is close to the valence

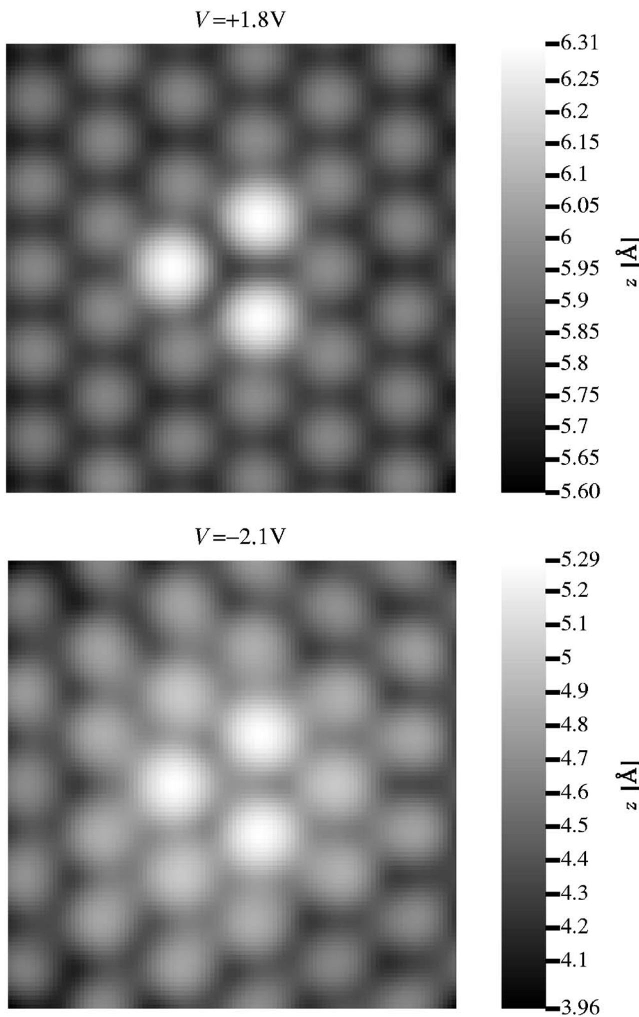

FIG. 9. Simulated STM images of the excess adsorbed chlorine. A $Si_{664}H_{189}Cl_{76}$ crystallite model was used for the simulations (see Fig. 10). The figures cover an area of 10×10 Å^2, showing most of the top surface of the crystallite. The bars on the right show the scale for height z. The height scales have been optimized to the highest and lowest values found in each image. The topmost silicon layer is at $z=0$. The electronic eigenstates were populated according to a temperature of 300 K. The excess adsorbed chlorine atom is at the very center of each picture, but it is not directly visible although some effects of its presence are. Upper panel: Tip bias $V=+1.8$ V, current $I=12$ μA. Imaging of filled states shows that the three Cl atoms surrounding the excess Cl atom appear to stand out by $\sim$0.3 Å above the other Cl atoms on the surface. Lower panel: Tip bias $V=-2.1$ V, current $I=240$ nA. Imaging of empty states shows height enhancement over a wider region than for positive bias, reflecting the spatial extent of the acceptor state bound to the excess Cl atom.

band edge at the surface. In comparing this STM simulation with an actual experiment, we have to consider how the actual voltage and current are measured. The n-doped bulk of the substrate and the acceptor impurities at the surface create a p-n junction. The voltage and current in the simulation are calculated between the tip and the hole gas at the surface of the subtrate, while an experiment would measure the voltage and current between the tip and the bulk of the substrate, that is, across both the tip-substrate point contact and the p-n junction. We would therefore expect images similar to those shown in Fig. 9 to be found at larger voltages and smaller currents in an experiment than in the STM simulation.

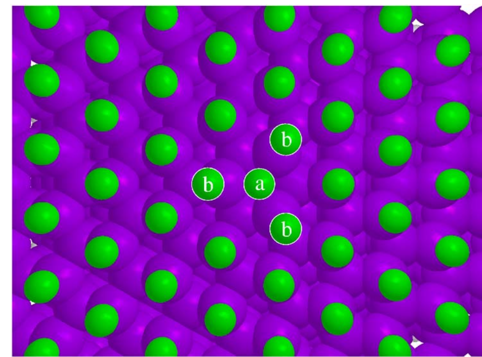

FIG. 10. (Color online) Illustration of the actual positions of atoms on the surface of the $Si_{664}H_{189}Cl_{76}$ crystallite used in the STM image simulation (see Fig. 9). The excess adsorbed Cl atom, marked a, is situated 0.65 Å below the unperturbed surface Cl atoms. The three nearest-neighbor Cl atoms, marked b, are situated 0.1 Å above the unperturbed surface Cl atoms (see also Fig. 7 and Table I). (Cl atoms are green, Si atoms are purple.)

In imaging of filled states (see upper panel), the three Cl atoms adjacent to the excess Cl atom appear to stand out about 0.3 Å above the rest of the surface Cl atoms the actual physical height of these adjacent Cl atoms is 0.1 Å above the rest of the chlorine surface atoms (see Table I). We find that the apparent height of the three adjacent Cl-atoms above the other surface atoms is largest at the smallest possible imaging bias but the general picture is quite insensitive to the applied voltage. The apparent height is mostly due to excess charging of the atomic orbitals on these three sites. The excess Cl atom is situated 0.76 Å below the three surrounding Cl atoms and is effectively masked by their presence. The three adjacent Cl atoms are displaced 0.7 Å radially by the presence of the excess Cl atom. The number of states within 1.8 eV of the valence band top is very large and filled states imaging renders a picture averaged over this large number of states. This averaged image should therefore be less sensitive to the details of the states at the valence band edge than imaging based on few states.

In imaging of empty states (see lower panel of Fig. 9), we see a broader feature. This image show the acceptor state bound to the defect site. Because this feature is based on fewer states than the filled states imaging, we require a more detailed analysis of what an experiment may show. There are several things to consider here. The acceptor state is confined by the small crystallite; we calculated in Sec. IV F the Bohr radius of the acceptor state in a macroscopic crystal. The twofold-degenerate acceptor state has an occupancy including spin of 3.05 electrons in this small crystallite at 300 K; in a macroscopic sample with a smaller acceptor state energy, this would of course be higher (more electrons excited into the acceptor state), but even at a small acceptor energy of 100 meV the occupancy of this state will not exceed 3.5 electrons. The feature shown in the lower panel of Fig. 9 would therefore be wider and weaker, mainly due to the ex-

panded wave function, in a macroscopic sample. The hole gas created by the acceptor has a very small density on the surface Cl atoms and we find that a fairly large negative bias is required, allowing tunneling into the conduction band, for imaging on this surface in areas away from the impurity. Since this feature is due to a state near the valence band and the background is due to tunneling into the conduction band it will be most prominent at the smallest bias for which imaging is possible. We also note that this small crystallite has a band gap of 1.8 eV due to the confinement effect and the −2.1 V bias used here would correspond to a bias of −1.4 V on a macroscopic surface.

VI. CONCLUSIONS

We have theoretically examined the Si(111):Cl surface in order to explain a recent experiment which shows a hole gas to form at this surface. We find that this hole gas, contrary to a previously proposed explanation, is not intrinsic to the Si(111):Cl surface but must be due to an acceptor defect or impurity. The low density of the hole gas also is indicative of an extrinsic origin for the free carriers. Further, we have examined a number of possible candidates for this acceptor and we find that only the ionic adsorption of excess Cl atoms at the surface fits the electronic character. We estimate the energy of the acceptor state to be between 45 and 100 meV. We have also performed STM simulations in order to investigate how the excess adsorbed Cl atoms will appear in a STM experiment.

ACKNOWLEDGMENTS

We thank K. Kavanagh for discussions. This work was supported by NSERC and the Canadian Institute for Advanced Research.

*Electronic address: tblomqui@sfu.ca
†Electronic address: kirczeno@sfu.ca

[1] G. Kirczenow, P. G. Piva, and R. A. Wolkow, Phys. Rev. B **72**, 245306 (2005).
[2] P. G. Piva, G. A. DiLabio, J. L. Pitters, J. Zikovsky, M. Rezeq, S. Dogel, W. A. Hofer, and R. A. Wolkow, Nature (London) **435**, 658 (2005).
[3] G. P. Lopinski, D. D. M. Wayner, and R. A. Wolkow, Nature (London) **406**, 48 (2000).
[4] A. J. Mayne, M. Lastapis, G. Baffou, L. Soukiassian, G. Comtet, L. Hellner, and G. Dujardin, Phys. Rev. B **69**, 045409 (2004).
[5] M. A. Phillips, J. N. O'Shea, P. R. Birkett, J. Purton, H. W. Kroto, D. R. M. Walton, R. Taylor, and P. Moriarty, Phys. Rev. B **72**, 075426 (2005).
[6] G.-C. Liang and A. W. Ghosh, Phys. Rev. Lett. **95**, 076403 (2005).
[7] A. Hermann, W. G. Schmidt, and F. Bechstedt, Phys. Rev. B **71**, 153311 (2005).
[8] S. Rangan, J.-J. Gallet, F. Bournel, S. Kubsky, K. Le Guen, G. Dufour, F. Rochet, F. Sirotti, S. Carniato, and V. Ilakovac, Phys. Rev. B **71**, 165318 (2005); **71**, 165319 (2005).
[9] S. Rangan, S. Kubsky, J.-J. Gallet, F. Bournel, K. Le Guen, G. Dufour, F. Rochet, R. Funke, M. Kneppe, G. Piaszenski, U. Köhler, and F. Sirotti, Phys. Rev. B **71**, 125320 (2005).
[10] M. Dubois, C. Delerue, and G. Allan, Phys. Rev. B **71**, 165435 (2005).
[11] T. Rakshit, G. C. Liang, A. W. Ghosh, M. Hersam, and S. Datta, Phys. Rev. B **72**, 125305 (2005).
[12] H. S. Stoker, *Introduction to Chemical Principles*, 4th ed. (Macmillan, New York, 1993).
[13] C. Kittel, *Introduction to Solid State Physics*, 7th ed. (Wiley and Sons, New York, 1996).
[14] G. P. Lopinski, B. J. Eves, O. V. Hul'ko, C. Mark, S. N. Patitsas, R. Boukherroub, and T. R. Ward, Phys. Rev. B **71**, 125308 (2005).
[15] T. Blomquist and G. Kirczenow, Nano Lett. **4**, 2251 (2004).
[16] T. Blomquist and G. Kirczenow, Nano Lett. **6**, 61 (2006).
[17] T. Blomquist and G. Kirczenow, Phys. Rev. B **71**, 045301 (2005).
[18] K. Yates, *Hückel Molecular Orbital Theory* (Academic, New York, 1978).
[19] V. Fiorentini, Phys. Rev. B **46**, 2086 (1992).
[20] S. P. McGlynn, L. G. Vanquickenborne, M. Kinoshita, and D. G. Carroll, *Introduction to Applied Quantum Chemistry* (Holt, Rinehart and Winston, New York, 1972).
[21] J. H. Ammeter, H.-B. Bürgi, J. C. Thibeault, and R. Hoffmann, J. Am. Chem. Soc. **100**, 3686 (1978); M.-H. Whangbo and R. Hoffmann, J. Chem. Phys. **68**, 5498 (1978).
[22] W. A. Harrison, *Electronic Structure and the Properties of Solids* (Dover, New York, 1989).
[23] I. I. Guseinov, J. Phys. B **3**, 1399 (1970).
[24] N. Bernstein, M. J. Mehl, D. A. Papaconstantopoulos, N. I. Papanicolaou, M. Z. Bazant, and E. Kaxiras, Phys. Rev. B **62**, 4477 (2000); **65**, 249902(E) (2002).
[25] M. Lannoo, C. Delerue, and G. Allan, Phys. Rev. Lett. **74**, 3415 (1995).
[26] M. Schlüter, J. E. Rowe, G. Margaritondo, K. M. Ho, and M. L. Cohen, Phys. Rev. Lett. **37**, 1632 (1976).
[27] R. I. G. Uhrberg and G. V. Hansson, CRC Crit. Rev. Solid State Mater. Sci. **17**, 133 (1991).
[28] R. D. Schnell, D. Rieger, A. Bogen, F. J. Himpsel, K. Wandelt, and W. Steinmann, Phys. Rev. B **32**, 8057 (1985).
[29] P. K. Larsen, N. V. Smith, M. Schlüter, H. H. Farrell, K. M. Ho, and Marvin L. Cohen, Phys. Rev. B **17**, 2612 (1978).
[30] M. Schlüter and M. L. Cohen, Phys. Rev. B **17**, 716 (1978).
[31] K. Mednick and C. C. Lin, Phys. Rev. B **17**, 4807 (1978).
[32] J. E. Rowe, G. Margaritondo, and S. B. Christman, Phys. Rev. B **16**, 1581 (1977).
[33] P. J. Feibelman, E. J. McGuire, and K. C. Pandey, Phys. Rev. B **17**, 1799 (1978).
[34] F. Illas, J. Rubio, and J. M. Ricart, Phys. Rev. B **31**, 8068 (1985).
[35] B. N. Dev, K. C. Mishra, W. M. Gibson, and T. P. Das, Phys. Rev. B **29**, 1101 (1984); S. M. Mohapatra, B. N. Dev, K. C. Mishra, N. Sahoo, W. M. Gibson, and T. P. Das, *ibid.* **38**, 12556 (1988).
[36] M. Seel and P. S. Bagus, Phys. Rev. B **28**, 2023 (1983).

[37] P. H. Citrin, J. E. Rowe, and P. Eisenberger, Phys. Rev. B **28**, 2299 (1983).
[38] J. J. Boland and J. S. Villarrubia, Phys. Rev. B **41**, 9865 (1990).
[39] J. S. Villarrubia and J. J. Boland, Phys. Rev. Lett. **63**, 306 (1989).
[40] S. Rivillon, R. T. Brewer, and Y. J. Chabal, Appl. Phys. Lett. **87**, 173118 (2005).
[41] L. S. O. Johansson, R. I. G. Uhrberg, R. Lindsay, P. L. Wincott, and G. Thornton, Phys. Rev. B **42**, 9534 (1990).
[42] G. A. de Wijs and A. Selloni, Phys. Rev. B **64**, 041402(R) (2001).
[43] K. Nakayama, C. M. Aldao, and J. H. Weaver, Phys. Rev. Lett. **82**, 568 (1999).
[44] G. A. de Wijs and A. Selloni, Phys. Rev. Lett. **77**, 881 (1996).
[45] G. Xu, E. Graugnard, V. Petrova, Koji S. Nakayama, and J. H. Weaver, Phys. Rev. B **67**, 125320 (2003); G. J. Xu, K. S. Nakayama, B. R. Trenhaile, C. M. Aldao, and J. H. Weaver, *ibid.* **67**, 125321 (2003); G. J. Xu, S. V. Khare, K. S. Nakayama, C. M. Aldao, and J. H. Weaver, *ibid.* **68**, 235318 (2003); G. J. Xu, N. A. Zarkevich, A. Agrawal, A. W. Signor, B. R. Trenhaile, D. D. Johnson, and J. H. Weaver, *ibid.* **71**, 115332 (2005).
[46] D. Chen and J. J. Boland, Phys. Rev. B **67**, 195328 (2003); **70**, 205432 (2004).
[47] J. Y. Lee and M.-H. Kang, Phys. Rev. B **69**, 113307 (2004).
[48] Q. Zhang, J. Costa, and E. Bertran, Phys. Rev. B **53**, 7847 (1996).
[49] L.-Q. Lee and P.-L. Cao, J. Phys.: Condens. Matter **6**, 6169 (1994).
[50] P. J. vandenHoek, W. Ravenek, and E. J. Baerends, Phys. Rev. B **38**, 12508 (1988).
[51] G. A. de Wijs, A. De Vita, and A. Selloni, Phys. Rev. B **57**, 10021 (1998).
[52] C. Nordling and J. Österman, *Physics Handbook*, 6th ed. (Studentlitteratur, Lund, Sweden, 1999).
[53] We employed the GAUSSIAN 98 numerical implementation of the Austin Model 1 (AM1) Hamiltonian to calculate the relaxed geometry.
[54] D. J. Chadi, Appl. Phys. Lett. **71**, 806 (1997).
[55] H. Runge, IEEE Trans. Electron Devices **11**, 1233 (1976).
[56] F. Bechstedt and R. Del Sole, Solid State Commun. **74**, 41 (1990).
[57] P. C. W. Davies and D. S. Betts, *Quantum Mechanics*, 2nd ed. (Chapman and Hall, London, 1994).
[58] O. Madelung, *Semiconductors Group IV Elements and III-V Compounds* (Springer-Verlag, Berlin, 1991).
[59] J. Tersoff and D. R. Hamann, Phys. Rev. Lett. **50**, 1998 (1983).
[60] S. Datta, *Electronic Transport in Mesoscopic Systems* (Cambridge University Press, Cambridge, UK, 1998).
[61] L. F. Mattheiss and D. R. Hamann, Phys. Rev. B **29**, 5372 (1984), Fig. 4. Mattheiss and Hamann's figure shows a value of 1.5 $\text{at.}^{-1}\,\text{eV}^{-1}$ at the Fermi energy for the W surface, but there is a difference in how spin is handled; they have plotted the density of spin states, while we use the density of spin-degenerate states.
[62] While methods based on supercells and periodic boundary conditions could be used to overcome confinement effects in models with a small number of atoms they cannot be used to study single impurities since localized impurity states would be turned into continuous energy bands.
[63] We find the values of the radical surface site state energies, relative to the nearest band edge, to be within 20% of the values for the H-terminated surface.